SUPPLEMENTARY INFORMATION

Drought self-propagation in drylands due to land–atmosphere feedbacks

Dominik L. Schumacher[1], Jessica Keune[1], Paul Dirmeyer[2], Diego G. Miralles[1]

[1]Hydro-Climate Extremes Lab, Ghent University, Ghent, Belgium
[2]Center for Ocean-Land-Atmosphere Studies, George Mason University, Fairfax, Virginia, USA

Supplementary Table 1: All 40 recent drought events selected for analysis.

ranking	main regions (non-exhaustive)	time period
1	Western Russia and Kazakhstan	May 2009 – Aug 2013
2	Eastern Europe and western Russia	May 2014 – Sep 2015
3	Eastern Russia, Mongolia, and Manchuria	Jul 2006 – Feb 2009
4	Central Africa	Apr 2015 – Oct 2016
5	D. R. of the Congo	Apr 2013 – Oct 2016
6	Siberia, Russian Far East	Aug 2013 – Oct 2016
7	Great Plains, midwestern & southeastern U.S.	Aug 1987 – Nov 1990
8	Gran Chaco, Pampas	Feb 2008 – Aug 2009
9	Central Africa, D. R. of the Congo	Nov 2003 – May 2007
10	Eastern Russia, Mongolia, and Manchuria	Jul 2000 – Oct 2003
11	Southern Africa	Dec 1991 – May 1993
12	Northwestern Russia	May 1988 – Oct 1989
13	Amazonia	Jul 1997 – Feb 1998
14	Northern Siberia	Jun 2012 – Feb 2014
15	Caatinga	Oct 1990 – May 1993
16	Amazonia	Sep 1982 – Oct 1983
17	Southern and eastern Australia	Feb 2002 – Jan 2003
18	Mongolia, Xinjiang	Dec 1994 – Jan 1999
19	Amazonia, Central West Brazil	Oct 2014 – May 2016
20	Russian Far East	Jun 1991 – Oct 1992
21	Tibetan Plateau, Xinjiang	Nov 1983 – Mar 1986
22	Southern Africa	Nov 1982 – Apr 1983
23	Great Plains, midwestern U.S.	Mar 2012 – Mar 2013
24	Kazakhstan, Turkmenistan, Uzbekistan	Dec 1997 – Apr 1999
25	Gran Chaco, Pantanal	Jun 2011 – Aug 2013
26	Northwestern and central Australia	Jan 2005 – May 2005

27	Western and central Australia	Jan 2008 – Jul 2008
28	Northern Mexico, southwestern U.S.	Oct 2010 – Oct 2011
29	Canadian Prairie	Nov 2000 – Sep 2002
30	Central and northern Australia	Jan 1986 – Apr 1986
31	Sahel	May 1984 – Sep 1984
32	Northwestern Russia	Aug 2001 – Jan 2003
33	Sudan, South Sudan, Ethiopia, Kenya, Tanzania	Jan 2009 – Oct 2009
34	Southern China, Myanmar	Aug 2003 – Apr 2004
35	Namibia, Botswana, Zambia, Mozambique	Dec 1994 – May 1995
36	Southeastern Australia	May 1982 – Dec 1982
37	Botswana, Zambia, Zimbabwe, Mozambique	Jan 1987 – Apr 1987
38	Continental southeast Asia	Oct 2004 – May 2005
39	Southern China	Aug 2009 – May 2010
40	Nigeria, Niger, Chad, Sudan	May 1983 – Nov 1983

Additional Figures

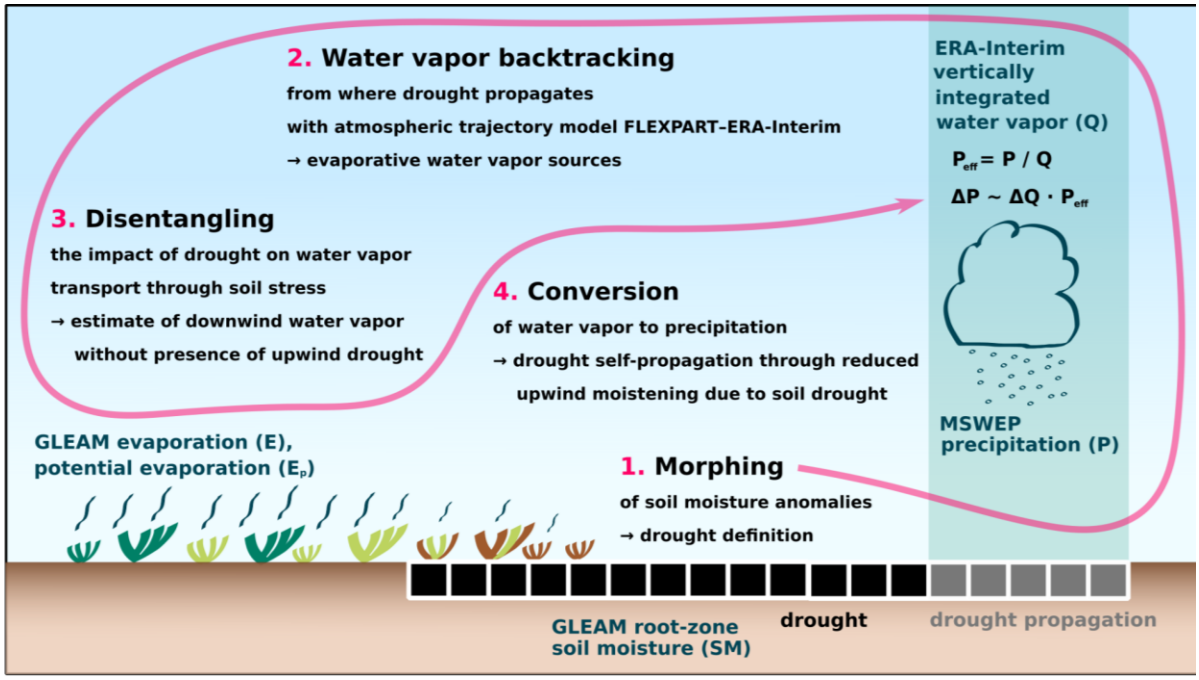

SFig. 1: Overview of the main methodological steps to estimate drought self-propagation. The large pink arrow represents the sequence of the steps (1–4), and text in dark blue font indicates input datasets. After applying the morphing procedure (1.) to root-zone soil moisture anomalies, vertically integrated water vapor (Q) is tracked backwards in time from all areas where the drought propagates (2.), yielding upwind moisture sources and corresponding source–receptor relationships. For the upwind sources already subject to the same spatiotemporally coherent drought event, the downwind reduction in water vapor, ΔQ, caused by anomalous soil stress (S') is calculated (3.). At last (4.), this reduction in water vapor is converted to a reduction in precipitation ΔP using the observed precipitation efficiency, resulting in an estimate of drought self-propagation solely through soil moisture limitations in upwind tropospheric moistening. This represents the impact of the land surface on downwind precipitation in the absence of land-induced alterations to precipitation efficiency.

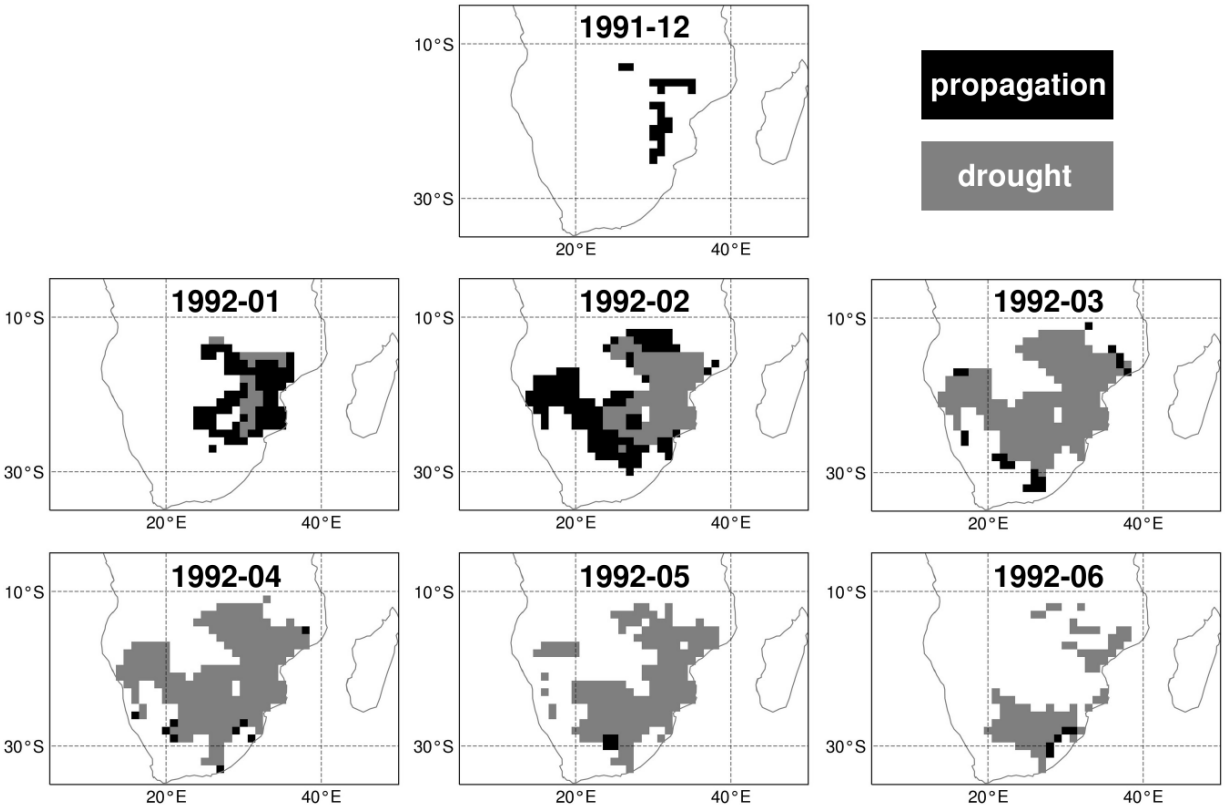

SFig. 2: Example of a morphed drought event based on monthly root-zone soil moisture anomalies. The key evolution of the drought is shown, from onset (1991-12) to nearly offset (after 1992-06, only a few morphed drought pixels remain for a few months). Black pixels indicate areas where the drought onset has just occurred (= propagation), whereas grey pixels denote regions in which the drought still persists at the given month. Every pixel may be considered as part of a propagation step only once during each drought event.

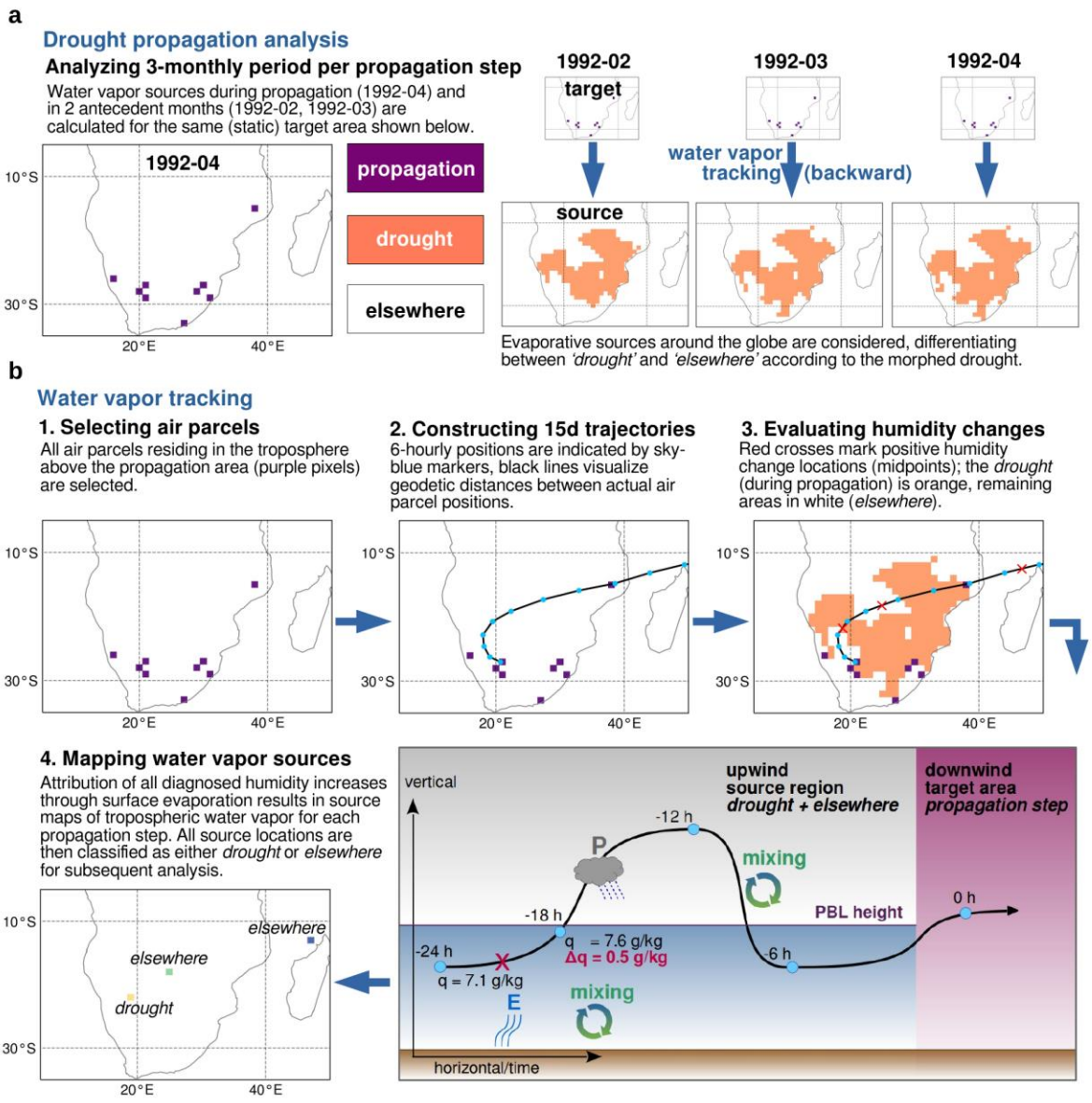

SFig. 3: Propagation steps and water vapor tracking. a, For drought propagation occurring in 1992-04 (purple pixels), all tropospheric water vapor of the same month is tracked back in time, and also the water vapor that resided over the same target area during the two antecedent months, here 1992-03 and 1992-02, taking soil memory into account. This is performed as such for all propagation steps of all droughts, so that water vapor above the same propagation area is tracked backwards for a total of 3 months, and the source distinction between *drought* and *elsewhere* is based on the respective state of the morphed drought (orange pixels). **b**, Visualization of backward tracking for water vapor residing over the selected propagation area during the month of propagation, 1992-04. Note that steps 1–4 shown here are executed thrice per propagation step, as visualized in **a**.